Bull. Chem. Soc. Jpn., 70, 89—95 (1997)

A New Method of Determining the Rate Constants for State-to-state Vibrational Relaxation: An Integrated Profiles Method

Katsuyoshi Yamasaki* **and Akihiro Watanabe**

Department of Chemistry, Niigata University, 2-Nocho, Ikarashi, Niigata 950-21

(Received August 5, 1996)

A new method of analysis for determining the rate constants of vibrational relaxation has been developed. Linearization of the equations of regression makes it possible to resolve the various problems and disadvantages of the conventional non-linear least-squares analyses. Not only the rate constants but also the relative detection sensitivities of different vibrational levels can be determined without information on photochemical parameters by which excitation spectra are usually corrected. Consequently, nascent vibrational distributions of the molecules produced in photolyses or chemical reactions can also be determined from the profiles recorded even under multiple collision conditions. The principles of the new method and how some advantage is offered are described, along with the comparison with the conventional analyses. Application of the method to practical schemes is also shown in detail.

Laser spectroscopy has been used to great advantage not only in the fields of reaction dynamics but also in those of chemical kinetics.[1—3] Study of the chemistry of non-emissive electronic states — a typical example is an electronic ground state — has been greatly advanced by the use of lasers. Not only reactions but also vibrational energy transfers have been important subjects of extensive experiments for a long time.[4] Since a single quantum level can be observed by laser-based techniques, for example laser-induced fluorescence (LIF)[5] and multiphoton ionization (MPI),[6,7] studies on state specific vibrational energy transfer have made great progress.

Temporal profiles of all the vibrational levels associated with energy transfer must be observed and analyzed to extract the information on the rate constant for each level. An ordinary way of analysis is non-linear fit by analytical solutions or numerical integration of rate equations. Fitting parameters are determined so that observed profiles are reproduced well. An initial trial set of parameters of concentrations and rate constants have to be given prior to the ordinary analyses. Unfortunately, results frequently depend on the initial trial set of parameters; therefore, rate constants are not always determined unequivocally. A new method is introduced in this paper to resolve the problems of the conventional analyses. Since regression equations are linearized, parameters in the analysis, i.e., rate constants and relative detection sensitivities, are determined unambiguously.

A knowledge of relative populations among vibrational levels is helpful in some cases to perform non-linear analyses. Laser-induced fluorescence excitation spectra are usually recorded to obtain vibrational distributions of the molecules of interest. In the analysis of the spectra, various factors related to photochemical properties of the molecules have to be applied for correcting the spectra.[8,9] Franck–Condon factors and the dependence of transition dipole moment on the vibrational levels (r-centroid dependence of transition dipole) have to be taken into account to derive correct intensities of the transitions. In addition, information on the dependence of fluorescence quantum yield of each rotational line observed is also indispensable for correction. Furthermore, rates of predissociation and quenching, which reduce the LIF intensity, are known to depend on rotational quantum numbers.[10—13] If fluorescence lifetimes are different among rotational levels, the overlap between fluorescence decay curves and the sampling gate of an integrator (fixed boxcar) should also be corrected.[14] Optical filters are frequently used in LIF experiments to block the stray light of the photolysis and probe lasers. Since spectral distributions of the fluorescence from different vibrational levels are not the same, the overlap between the fluorescence and the filters used has to be corrected. Unfortunately, there are few cases in which all the precise factors described above are available.

Not only the rate constants of vibrational relaxation but also relative detection sensitivities are obtained simultaneously in the analysis introduced in this paper. Since the time-evolutions of relative concentrations among all the levels are obtained, the initial relative populations on the levels as the products of preceding photolysis or reaction can be determined. The difference between the present method and the conventional analyses will be shown and how the method is to be applied to realistic systems will be described in detail.

Conventional Non-Linear Analyses

First, consider a process of vibrational relaxation

$$A \xrightarrow{k_1} B \xrightarrow{k_2} C, \qquad (1)$$

where A, B, and C are different vibrational levels: for example A represents a vibrational level $v=2$, B is $v=1$, and C is $v=0$. As often seen in textbooks,[14—16] temporal profiles of the concentrations of each species are given under the initial conditions: $[A]_{t=0}=[A]_0, [B]_{t=0}=[C]_{t=0}=0$

$$[A] = [A]_0 \exp(-k_1 t), \tag{2}$$

$$[B] = \frac{k_1[A]_0}{k_1 - k_2}[\exp(-k_2 t) - \exp(-k_1 t)], \tag{3}$$

$$[C] = [A]_0\left\{1 - \frac{1}{k_1 - k_2}[k_1 \exp(-k_2 t) - k_2 \exp(-k_1 t)]\right\}. \tag{4}$$

The initial concentrations except $[A]_0$ are zero for the sake of simplicity and this assumption loses neither rigorousness nor generality. Concentration of A shows a single-exponential decay and that of B shows double-exponential profile with growth and decay. The rate constant k_1 is determined by an ordinary semilogarithmic plot of [A] vs. t. Another rate constant k_2 seems to be obtained from a semilogarithmic plot of [B] at large t over which $\exp(-k_2 t)$ is sufficiently larger than $\exp(-k_1 t)$. This type of analysis, however, is possible only when $k_1 > k_2$. It should be noted that the terms $\exp(-k_1 t)$ and $\exp(-k_2 t)$ do not always govern decay and growth, respectively. If $k_1 < k_2$, not k_2 but k_1 is derived from the semilogarithmic plot of the decay part of [B].

The intensity of a signal is not readily converted to an absolute concentration even when the intensity is proportional to the absolute concentration. Thus, unknown proportionality constants are always present to associate the observed signal intensities with absolute concentrations, for example $I_A = \alpha[A]$, where I_A represents the observed signal intensity of LIF or MPI due to a single rotational transition of the species A, and α is a proportionality constant (detectivity of the apparatus) for the species A. As long as rotational motion is equilibrated with the ambient temperature, the population on each vibrational level of interest can be monitored by a signal due to a rotational transition. When the absolute concentrations in Eq. 3 are replaced with corresponding signal intensities, $I_A = \alpha[A]$ and $I_B = \beta[B]$, the following equation is obtained

$$I_B = \frac{\beta}{\alpha}\frac{k_1 I_{A_0}}{k_1 - k_2}[\exp(-k_2 t) - \exp(-k_1 t)], \tag{5}$$

where I_{A_0} is a signal intensity of A at $t=0$ and the factor β/α is the relative sensitivity of the species A and B. Since the relative sensitivity β/α is unknown, not only rate constants but also a scaling factor must be determined in the analysis. Because the time dependence of the profile of B is represented by the term $\exp(-k_2 t) - \exp(-k_1 t)$, and growth always corresponds to the faster process and decay corresponds to the slower one in Scheme 1, the observed profile I_B is fit to the following form:

$$I_B = C[\exp(-k_{\text{decay}} t) - \exp(-k_{\text{growth}} t)] \quad (C > 0), \tag{6}$$

using non-linear double-exponential least-squares fit.[17—19] Even when k_{growth} and k_{decay} are determined by the analysis using Eq. 6, there is no way to decide which of k_{growth} or k_{decay} corresponds to k_1 or k_2 from only the analysis of I_B. Since the rate constant k_1 is separately determined by the profile (decay) of A, it seems to be possible to conclude whether k_{growth} or k_{decay} is k_1 or k_2. However, double-exponential analysis frequently fails to obtain correct k_{growth} and k_{decay} values, particularly when the rate constants are not much different. Carrington[20] gave a criterion for profiles to be reliably analyzed by the non-linear double-exponential least-squares fit:

$$|k_{\text{growth}} - k_{\text{decay}}| \cdot t_{\max} \geq 1, \tag{7}$$

where $t_{\max}$ is the maximum time over which the signal of B can be observed (that is, distinguished from background noise). Equation 7 indicates that the rate constants are not precisely determined from the profiles with $k_{\text{growth}} \approx k_{\text{decay}}$, because the actual signal at very large t is too weak to observe with good signal-to-nose (S/N) ratio. Therefore, the k_1 obtained from the profile of A is in agreement with neither k_{growth} nor k_{decay}, and thus k_2 cannot be determined. When a profile with k_1 a little larger than k_2 is analyzed, the order of magnitude of the rate constants is $k_{\text{decay}} < k_2 < k_1 < k_{\text{growth}}$, as shown later.

The profile of B in Scheme 1 with rate constants $k_1 = 4.0\times10^3$ s^{-1} and $k_2 = 3.8\times10^3$ s^{-1} was synthesized as shown in Fig. 1(a) and analyzed by non-linear regression method. For simplicity, the initial concentration of B was set to be zero ($[B]_0=0$). First, non-linear least squares fit was performed on the assumption that k_{growth} and k_{decay} correspond to k_1 and k_2, respectively. The initial trial values of k_{growth} and k_{decay} for the iterative calculations have to be given with the greatest care, because results are dependent on the initial values in non-linear analysis. We shall henceforth write the initial values of k_{growth} and k_{decay} by k°_{growth} and k°_{decay} to avoid confusion. The value of k°_{decay} was first determined from a semilogarithmic plot ($\ln[B]$ vs. t) of the data shown in Fig. 1(a) over large t. In principle, a more accurate value of k°_{decay} is obtained from the slope at larger t; however, actually the signal observed at larger t cannot be analyzed because of noise on the data. When the S/N ratio is 10, the signal is below noise after the time at which the intensity is smaller than 1/10 of the maximum. The k°_{decay} was determined to be 2.439×10^3 s^{-1} from the slope of a semilogarithmic plot in the range of 0.5—1 ms. When the S/N ratio increased up to 100, the analysis of the data in the range from 1.5 ms to 2 ms gave k°_{decay} to be 3.300×10^3 s^{-1}. The value of k°_{growth}, on the other hand, was determined by the curve generated from Eq. 6 multiplied by a term $\exp(+k^\circ_{\text{decay}} t)$. The maximum value of the profile transformed from Eq. 6 was regarded as the asymptote in the determination of k°_{growth}, and the values of k°_{growth} were 6.839×10^3 s^{-1} and 4.992×10^3 s^{-1} for S/N=10 and 100, respectively. The initial value of the scaling factor C was so obtained that the maximum value of Eq. 6 was the same as that of the analyzed data. A resulting curve obtained using the initial parameters for S/N=100 with permissible error of 2 % is shown in Fig. 1(b). The curve appears to reproduce the data shown in Fig. 1(a); nevertheless, the rate constants finally obtained in the analysis, $k_{\text{growth}} = 4.655\times10^3$

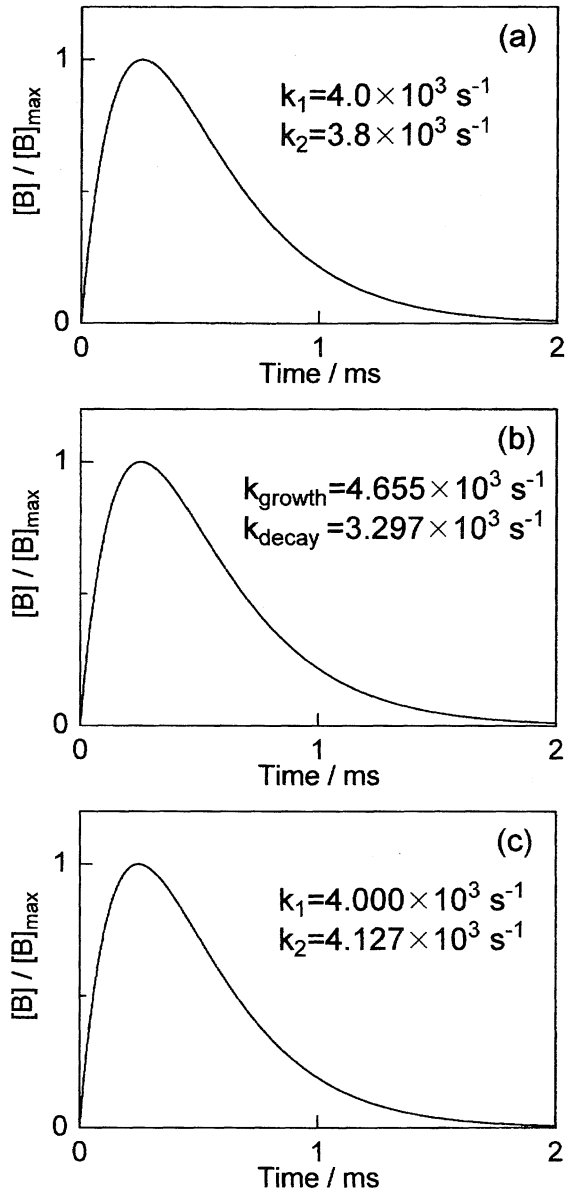

Fig. 1. Temporal profiles of the species B in a scheme of A→B→C. Each profile is normalized with its maximum value. (a) A synthetic profile of B with the rate constants: $k_1=4.0\times10^3$ s^{-1} for A→B and $k_2=3.8\times10^3$ s^{-1} for B→C; (b) A profile obtained by the non-linear double-exponential analysis: $k_{growth}=4.655\times10^3$ s^{-1} and $k_{decay}=3.297\times10^3$ s^{-1}; (c) A profile obtained by the optimization of the rate constant $k_2=4.127\times10^3$ s^{-1} with a fixed $k_1=4.000\times10^3$ s^{-1}. The initial trial set of the parameters were determined from semilogarithmic plot of the synthesized data over 1.5—2 ms on the assumption that S/N=100. The method introduced in the present paper gave perfect results: $k_1=3.9999\times10^3$ s^{-1} for A→B and $k_2=3.7999\times10^3$ s^{-1} for B→C and almost identical profile with that shown in (a).

s^{-1} and $k_{decay}=3.297\times10^3$ s^{-1}, diverge substantially from the correct rate constants $k_1=4.0\times10^3$ s^{-1} and $k_2=3.8\times10^3$ s^{-1}. The values obtained for S/N=10, $k_{growth}=4.657\times10^3$ s^{-1} and $k_{decay}=3.295\times10^3$ s^{-1}, are also significantly different from the correct values.

Another type of fit was performed to resolve the problem in non-linear double-exponential on the assumption that the rate constant k_1 was determined first by the analysis of the profile of A. Because the k_1 has to be in agreement with k_{growth} or k_{decay}, one of the rate constants in Eq. 6 was fixed to the value of k_1, after which the other rate constant and the factor C were optimized to reproduce the analyzed data. This type of analysis, however, also has a problem. Since the difference between k_1 and k_2 is not known, which of k_{growth} or k_{decay} corresponds to k_1 is not obvious. Naturally, the correct rate constant k_2 was obtained when the k_{growth} in Eq. 6 was replaced with k_1 in the analysis of the profiles with $k_1>k_2$ or the k_{decay} was replaced with k_1 for the profiles with $k_1<k_2$. When the profiles with correct rate constants $k_1>k_2$ were analyzed by Eq. 6 whose initial parameter of k_{decay} was assumed to be k_1, the resulting k_2 was incorrect. When the k_{decay} was replaced with k_1, the value of k_{growth} obtained by non-linear double-exponential analysis was adopted as k°_{growth}. Figure 1(c) shows the resulting curve obtained by the incorrect substitution, i.e., $k_{decay}=k_1$. The rate constants k_{growth} obtained are 4.127×10^3 s^{-1} for both S/N=10 and 100. The values are widely different from the correct k_2($=3.8\times10^3$ s^{-1}); nevertheless, the curves shown in Fig. 1(a) and Fig. 1(c) are too similar to distinguish any difference. Correlation coefficients of the curves in Fig. 2(b) and Fig. 2(c) are larger than 0.999. This fact indicates that non-linear fits are not effective particularly when the difference between k_1 and k_2 is not large.

When the k_1 is exactly the same as k_2 ($k_1=k_2=k$), Eq. 3 must be replaced by a different expression:

$$[B] = k[A]_0 t \exp(-kt). \tag{8}$$

Equation 8 is an mathematically asymptotic form of Eq. 3 as $(k_1-k_2)\rightarrow0$; however, the values of the Eq. 3 as $(k_1-k_2)\rightarrow0$ cannot be correctly evaluated by a computer, because both denominator and numerator are close to zero.

An Integrated Profiles Method

A new analysis introduced in the present paper will be described in this section. First, consider the analysis of time-dependent profiles of A, B, and C in Scheme 1. Integration of rate equations from $t=t_0$ to an arbitrary time t gives the following expressions:

$$[A] = [A]_0 - k_1 \int_{t_0}^{t} [A]dt, \tag{9}$$

$$[B] = [B]_0 + k_1 \int_{t_0}^{t} [A]dt - k_2 \int_{t_0}^{t} [B]dt, \tag{10}$$

$$[C] = [C]_0 + k_2 \int_{t_0}^{t} [B]dt, \tag{11}$$

where $[A]_0$, $[B]_0$, and $[C]_0$ are the concentrations of A, B, and C at $t=t_0$. How to decide appropriate lower limits (t_0) of the integrals will be described later. These equations appear to be trivial as solutions for rate equations from a mathematical point of view. They, however, offer a great advantage for the analysis of temporal profiles for schemes more complicated than Scheme 1. Analytical solutions Eqs. 3 and 4 are valuable to see the time evolution of concentrations of the species when the initial concentrations and

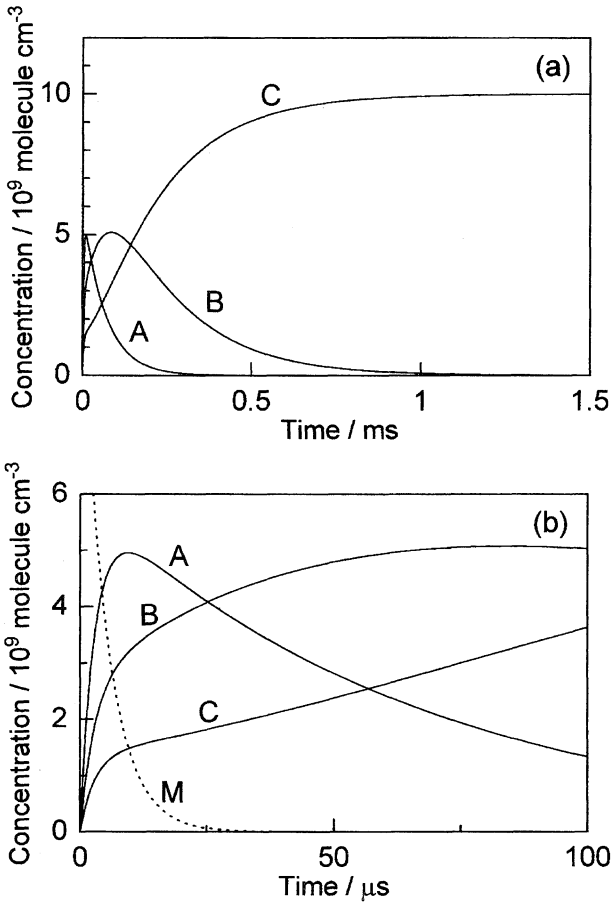

Fig. 2. Synthetic profiles of the species A, B, and C produced from a reaction of M (see Scheme 24). Rate constants for the reactions: $k_A^\circ=2\times10^5$ s^{-1} (M→A); $k_B^\circ=1\times10^5$ s^{-1} (M→B); and $k_C^\circ=5\times10^4$ s^{-1} (M→C). Rate constants for the relaxation $k_1=1.5\times10^4$ s^{-1} (A→B) and $k_2=5\times10^3$ s^{-1} (B→C). The initial conditions are $[M]_0=1\times10^{10}$ molecule cm^{-3} and $[A]_0=[B]_0=[C]_0=0$. (a) Profiles over the range of 0—1.5 ms; (b) Expanded profiles over the range of 0—100 μs. The profile of the reactant M is shown by the broken line.

rate constants are known. Equations 10 and 11, on the other hand, are useful in the analysis by which the rate constants and the initial populations of the levels are determined from temporal profiles observed in experiments. It is not difficult to calculate the integrals because the concentrations at each data point (i.e., time) can simply be summed up with a computer. A few significant characteristics of the equations should be noted. First, in contrast to the analysis using Eq. 3, simple linear regression is available to determine the rate constants unequivocally. Second, the ambiguity of the non-linear analysis can be eliminated not only because k_1 and k_2 cannot be exchanged in Eq. 10 but also because an initial trial set of parameters is not necessary. Third, Eq. 10 is always satisfied as long as the relation between A and B is represented by Scheme 1, even if the temporal profile of [A] in Eq. 10 is not given by a formula such as Eq. 2.

An additional feature is that the lower limits of the integrals of Eqs. 9, 10, and 11 are not $t=0$ but t_0. The signals at $t=0$ are not always necessary to determine the rate constants and the relative sensitivities. There are many unfortunate cases in which noise from the photolysis (or pump) laser at $t=0$ is so large that the signal at around $t=0$ is not reliable. A new arbitrary time t_0 ($\neq0$) can be chosen as the lower limit of the integrals in order to exclude the contaminated signals around $t=0$. The treatment is similar to that for the ordinary semilogarithmic analysis. The noise-free analysis determines reliable rate constants and newly defined "initial" intensities I_{A_0}, I_{B_0}, and I_{C_0} at t_0. Another type of problem can be resolved by the shifted lower limit of integration. Nascent rotational temperature of the molecules produced in the photolysis or reactions is not always equal to the ambient temperature. Rotational relaxation must be completed to monitor the concentration of a vibrational level by the signal due to a single rotational transition in LIF or MPI. Since rotational relaxation is much faster than vibrational relaxation,[1,4] an appropriate short delay for the lower limit of the integration (t_0) permits a reliable analysis without undesirable effects due to the non-thermalized rotation. Similarly, if the reaction producing vibrational levels A, B, and C is not completed instantaneously at $t=0$, the initial time of integration (t_0) can be placed at the time after termination of the reaction.

Furthermore, all the lower limits of the integrals do not have to be the same. The temporal profile of A, i.e., [A], which appears in Eq. 10 is the same as [A] in Eq. 9, whereas the lower limits of the integrals in Eqs. 10 and 11 may be different from that in Eq. 9. A different lower limits of the integrals offers an advantage in the analysis. There are some cases in which the level A shows growth immediately after $t=0$ because of relaxation from a higher level X that cannot be detected. The lower limit t_0 in Eq. 9 is defined as the initial time of the range over which the semilogarithmic plot [A] vs. t (see Eq. 2) or the plot [A] vs. $\int_{t_0}^{t}[A]dt$ (see Eq. 9) shows a straight line. Rate constant k_1 is determined from the slope. The lower limits t_0 in Eqs. 10 and 11 can be smaller than that in Eq. 9 as long as neither B nor C is directly produced from the X. The presence of X, which is a vibrational level higher than the observed highest level, does not lead to any uncertainty of the parameters in the rate constants and relative detectivities.

Recall that observed signal intensities are proportional to the concentrations, for example $I_A=\alpha[A]$. The concentrations in Eqs. 9, 10, and 11 have to be replaced with the signal intensities $I_A=\alpha[A]$, $I_B=\beta[B]$, and $I_C=\gamma[C]$, and the following equations are obtained:

$$I_A = I_{A_0} - k_1 \int_{t_0}^{t} I_A dt, \tag{12}$$

$$I_B = I_{B_0} + \frac{\beta}{\alpha} k_1 \int_{t_0}^{t} I_A dt - k_2 \int_{t_0}^{t} I_B dt, \tag{13}$$

$$I_C = I_{C_0} + \frac{\gamma}{\beta} k_2 \int_{t_0}^{t} I_B dt. \tag{14}$$

Note that the relative values among detection sensitivities (β/α and γ/β) are not known prior to the analysis. From a statistical point of view, k_1, $(\beta/\alpha)k_1$, k_2, and $(\gamma/\beta)k_2$ are partial regression coefficients, I_{A_0}, I_{B_0}, and I_{C_0} are constants, the integrals are independent variables, and I_A, I_B, and I_C are dependent variables. Since all the values of the partial regression coefficients are given by the multiple linear regression analysis, rate constants k_1, and k_2 and relative sensitivities β/α and γ/β are determined unequivocally. Analysis of the data shown in Fig. 1(a) by the present integrated profiles method gave correct rate constants ($k_1=3.9999\times10^3$ s^{-1} for A→B and $k_2=3.7999\times10^3$ s^{-1} for B→C) and a profile. The result is not shown because the curve obtained by the analysis is almost identical with the analyzed data. It was also confirmed that resulting parameters were independent of the temporal range of the analysis. The same rate constants and relative detectivities were actually obtained from the data within both 0—100 μs and 0—2

ms. Similarly, the results were the same when the data in the range of both 0—2 ms and 1.8—2 ms were analyzed.

When vibrational relaxation with $\Delta v=2$ cannot be neglected two paths (A→B and A→C) of relaxation from A must be taken into account, as shown in the following scheme:

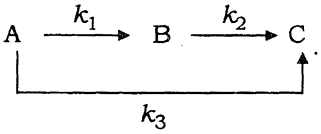

(15)

The branching ratio between k_1 and k_3 must be determined to reproduce the profiles of relative populations of all the levels. While conventional analyses based on non-linear fit are very complicated in this case, the present method enables us to readily obtain all the information on the rate constants and relative sensitivities among the species. Integrated rate equations for Scheme 15 are written as follows:

$$I_A = I_{A_0} - (k_1 + k_3)\int_{t_0}^{t} I_A dt, \tag{16}$$

$$I_B = I_{B_0} + \beta k_1 \int_{t_0}^{t} I_A dt - k_2 \int_{t_0}^{t} I_B dt, \tag{17}$$

$$I_C = I_{C_0} + \gamma k_3 \int_{t_0}^{t} I_A dt + \frac{\gamma}{\beta} k_2 \int_{t_0}^{t} I_B dt, \tag{18}$$

here α (detection sensitivity of A) is defined to be unity for simplicity. This treatment does not lose rigorousness, because not the absolute values but the ratios among α,β, and γ have to be determined in the analysis. First, I_{A_0} and k_1+k_3 are determined using Eq. 16. Then, time-independent parameters I_{B_0}, βk_1, and k_2 in Eq. 17, and I_{C_0}, γk_3 and $(\gamma/\beta)k_2$ in Eq. 18 are obtained by linear regression analysis. As a result, state-to-state rate constants k_1, k_2, and k_3 and the relative sensitivities β and γ are determined unequivocally from simultaneous equations composed of the parameters.

The present method can also be applied to schemes involving opposing reactions. For example, when the time-dependent profiles of the species A, B, and C in the following scheme are analyzed

$$A \underset{k_{-1}}{\overset{k_1}{\rightleftarrows}} B \underset{k_{-2}}{\overset{k_2}{\rightleftarrows}} C, \tag{19}$$

unequivocal determination of both forward and backward rate constants and relative sensitivities of the species is made from linear regression equations. The most general case of a system called a reaction network in which the following first-order reactions between any two components take place can be dealt with by the new method introduced in the present paper.

$$A_i \underset{k_{ji}}{\overset{k_{ij}}{\rightleftarrows}} A_j. \tag{20}$$

Because simultaneous equations composed of regression coefficients can be solved, all the rate constants and relative sensitivities are determined.

Thus far only closed systems from which no species are lost have been considered. It often happens in actual experiments that loss of species by diffusion or background reactions cannot be neglected. An example is shown by the following schemes:

$$A \longrightarrow B \longrightarrow C, \tag{21}$$

$$A, B, \text{ and } C \longrightarrow \text{Diffusion, reactions.} \tag{22}$$

If it can be assumed that the rate constants for the diffusion (or background reactions) called natural decay of A, B, and C are the same, rate constants of all the processes and relative detection sensitivities can be derived in the same manner as described in the previous examples. This assumption is appropriate when Scheme 21 represents vibrational relaxation and the loss is due only to diffusion, because diffusion rates for the molecules with the same mass might be very close. Even when natural decay is mainly due to reactions whose rate constants are different for A, B, and C, collisional (overall) removal rate constants of each species can be derived; however, the branching ratios between the processes in Scheme 21 and natural decay of each species cannot be determined without known relative detectivities. To be brief, the present method does not give respective values of rate constants, k_1 and k_2, and relative detectivities of A, B, and C in the following Scheme 23, in which two or more products are generated from a single reactant and the products do not have any relation.

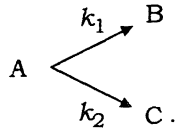

(23)

Only the overall rate constant, k_1+k_2, and relative detection sensitivities multiplied by each rate constant, $(\beta/\alpha)k_1$ and $(\gamma/\alpha)k_2$, are determined.

Determination of Nascent Vibrational Distributions

Ratios among the relative sensitivities, $\alpha:\beta:\gamma$, are independent of time because they are apparatus constants. Once the ratios are determined, time-evolution of relative concentrations on vibrational levels can be obtained. When the time constant of a preceding reaction is much shorter than that of a vibrational relaxation, all the vibrational levels are produced instantaneously like photolysis. In such cases, the initial vibrational distribution can be determined from the signal intensities at $t=0$ (I_{A_0}, I_{B_0}, and I_{C_0}). The initial relative populations of the vibrational levels, $[A]_0:[B]_0:[C]_0$ are given by $I_{A_0}/\alpha : I_{B_0}/\beta : I_{C_0}/\gamma = I_{A_0} : (\alpha/\beta)I_{B_0} : (\alpha/\gamma)I_{C_0}$.

However, the signal intensities at $t=0$ are not always determined precisely when the reaction is not sufficiently faster than the following relaxation. An example of such profiles is shown in Fig. 2(a). The profiles are synthesized according to the following Scheme 24:

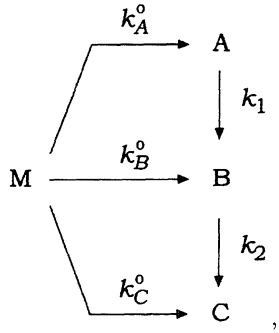

(24)

where M is a reactant converted to the product vibrational levels A, B, and C, and k_i° denotes a rate constant for the reaction M→i (i=A, B, and C). As can be seen in Fig. 2(b), the nascent relative vibrational populations of A, B, and C cannot be determined because of the overlap between the

timescales of the reaction and relaxation. Even in such cases, the initial population of each vibrational level can be obtained by the following analysis.

If the integrated profiles method is first applied to the observed profiles A, B, and C first, the rate constants for the relaxation (k_1 and k_2) are determined as described in the previous section. Since the relative sensitivities for A, B, and C are also obtained in the first analysis, profiles of relative concentrations can be drawn in a graph whose ordinate is common for all the vibrational levels, as shown in Fig. 2. The profile of M shows a single-exponential decay

$$[\mathrm{M}] = [\mathrm{M}]_0 \exp(-k^\circ t), \tag{25}$$

where k° ($=k_\mathrm{A}^\circ + k_\mathrm{B}^\circ + k_\mathrm{C}^\circ$) is an overall rate constant for the reaction of M, and $[\mathrm{M}]_0$ is the initial concentration of M. The rate equations for A, B and C in Scheme 24 are

$$\frac{\mathrm{d}[\mathrm{A}]}{\mathrm{d}t} = k_\mathrm{A}^\circ [\mathrm{M}]_0 \exp(-k^\circ t) - k_1[\mathrm{A}], \tag{26}$$

$$\frac{\mathrm{d}[\mathrm{B}]}{\mathrm{d}t} = k_\mathrm{B}^\circ [\mathrm{M}]_0 \exp(-k^\circ t) + k_1[\mathrm{A}] - k_2[\mathrm{B}], \tag{27}$$

$$\frac{\mathrm{d}[\mathrm{C}]}{\mathrm{d}t} = k_\mathrm{C}^\circ [\mathrm{M}]_0 \exp(-k^\circ t) + k_2[\mathrm{B}]. \tag{28}$$

Because the concentrations of A and B at both $t=0$ and $t=\infty$ are zero in Scheme 24, as seen in Fig. 2(a), the integrated value of the left-hand side of Eq. 26 from $t=0$ to $t=\infty$ is

$$\int_0^\infty \frac{\mathrm{d}[\mathrm{A}]}{\mathrm{d}t}\mathrm{d}t = \int_0^\infty \mathrm{d}[\mathrm{A}] = [\mathrm{A}]_\infty - [\mathrm{A}]_0 = 0. \tag{29}$$

The same equation is also satisfied for B. Therefore, the following equations are obtained after integration of both sides of Eqs. 26, 27, and 28 from $t=0$ to $t=\infty$:

$$\frac{k_\mathrm{A}^\circ [\mathrm{M}]_0}{k^\circ} = k_1 \int_0^\infty [\mathrm{A}]\mathrm{d}t, \tag{30}$$

$$\frac{k_\mathrm{B}^\circ [\mathrm{M}]_0}{k^\circ} = k_2 \int_0^\infty [\mathrm{B}]\mathrm{d}t - k_1 \int_0^\infty [\mathrm{A}]\mathrm{d}t, \tag{31}$$

$$\frac{k_\mathrm{C}^\circ [\mathrm{M}]_0}{k^\circ} = [\mathrm{C}]_\infty - k_2 \int_0^\infty [\mathrm{B}]\mathrm{d}t, \tag{32}$$

where $[\mathrm{C}]_\infty$ is the asymptotic concentration of C at $t=\infty$. Ratios among the rate constants (k_A°, k_B°, and k_C°) for the reactions producing specific vibrational levels can be obtained from the ratios among the values of Eqs. 30, 31, and 32. Because the time-dependent profiles are drawn with the common ordinate, the right-hand sides of the equations are calculated using the rate constants determined in the first analysis. A real analysis of the profiles shown in Fig. 2 gave a perfectly correct set of rate constants k_A°, k_B°, and k_C°. Neither the overall rate constant k° nor the initial concentration of M is necessary. The analysis described here can also be extended easily to the system containing more than three product vibrational levels.

There, however, is a defect of this method. If a part of the reaction products, A, B, and C in Scheme 24 are lost by reactions with unknown different rates, rate constants k_1 and k_2 cannot be obtained in the first analysis, as shown in the previous section. Accordingly, the calculations of the right-hand sides of Eqs. 30, 31, and 32 are not possible, and thus the present method cannot be applied to the system in which vibrationally excited products undergo not only vibrational relaxation but also chemical reactions.

Summary

A new kinetic analysis of time-dependent profiles has been developed. Regression equations are linearized by the method and several significant advantages are offered:

(1) Time-dependent profiles showing growth and decay whose rates are not widely different can be safely analyzed and correct rate constants are obtained.

(2) Relative detection sensitivities of different vibrational levels can be calibrated without photochemical information.

(3) Nascent vibrational distributions of the molecules produced in photolyses or reactions can be determined, even if the preceding processes do not terminate instantaneously.

The authors wish to thank Professor S. Koda and Mr. M. Sato for helpful discussions. Support for this research from the Ministry of Education, Science, Sports and Culture by the Grant-in-Aid for Scientific Research on Priority Areas "Free Radical Science" (Contract No. 05237106) and the Grant-in-Aid for Scientific Research (B) (Contract No. 08454181) is gratefully acknowledged.

References

1) R. D. Levine and R. B. Bernstein, "Molecular Reaction Dynamics and Chemical Reactivity," Oxford University Press, Oxford (1987).

2) W. Demtröder, "Laser Spectroscopy," 2nd ed, Springer-Verlag, Heidelberg (1982).

3) S. H. Lin, Y. Fujimura, H. J. Neusser, and E. W. Schlag, "Multiphoton Spectroscopy of Molecules," Academic Press, New York (1984).

4) J. T. Yardley, "Introduction to Molecular Energy Transfer," Academic Press, New York (1980).

5) R. N. Zare and P. J. Dagdigian, *Science*, **185**, 739 (1974).

6) E. E. Marinero, C. T. Rettner, and R. N. Zare, *Phys. Rev. Lett.*, **48**, 1323 (1982).

7) E. E. Marinero, R. Vasudev, and R. N. Zare, *J. Chem. Phys.*, **78**, 692 (1983).

8) W. Hack and Th. Mill, *J. Phys. Chem.*, **97**, 5599 (1993).

9) K. Honma, *J. Chem. Phys.*, **99**, 7677 (1993).

10) K. Yamasaki and S. R. Leone, *J. Chem. Phys.*, **90**, 964 (1989).

11) D. R. Crosley, *J. Phys. Chem.*, **93**, 6273 (1989).

12) E. L. Chappell, J. B. Jeffries, and D. R. Crosley, *J. Chem. Phys.*, **97**, 2400 (1992).

13) D. E. Heard, D. R. Crosley, J. B. Jeffries, G. P. Smith, and A. Hirano, *J. Chem. Phys.*, **96**, 4366 (1992).

14) C. Capellos and B. H. Bielski, "Kinetic Systems," Wiley-Interscience, New York (1972).

15) S. W. Benson, "The Foundations of Chemical Kinetics, " Robert E. Krieger, Malabar (1982).

16) K. J. Laidler, "Chemical Kinetics," 3rd ed, Harper & Row, Scranton (1987).

17) S. G. Cheskis, A. A. Iogansen, P. V. Kulakov, O. M. Sarkisov, and A. A. Titov, *Chem. Phys. Lett.*, **143**, 348 (1988).

18) S. G. Cheskis, A. A. Iogansen, P. V. Kulakov, I. Y. Razuvaev, O. M. Sarkisov, and A. A. Titov, *Chem. Phys. Lett.*, **155**, 37 (1989).
19) A. A. Iogansen, O. M. Sarkisov, E. V. Zimont, J. A. Seetula, R. S. Timonen, and S. Cheskis, *Chem. Phys. Lett.*, **212**, 604 (1993).
20) T. Carrington, *Int. J. Chem. Kinet.*, **14**, 517 (1982).